Incremental method of Young's modulus updating procedure in topology optimization

Ryszard Kutyłowski[1] **and Bartosz Rasiak**[2]

[1]*Institute of Civil Engineering, Wrocław University of Technology*
Wyb. Wyspiańskiego 27, 50-370 Wrocław, Poland
e-mail: ryszard.kutylowski@pwr.wroc.pl

[2]*Institute of Civil Engineering, Wrocław University of Technology*
Wyb. Wyspiańskiego 27, 50-370 Wrocław, Poland
e-mail: bartosz.rasiak@pwr.wroc.pl

Abstract

This paper presents a new Young modulus updating procedure as an extension to the SIMP method used for topology optimization. In essence, the new Young modulus updating procedure consists in taking into account in a given optimization step not only the material density from the preceding step, but also the increment in density in the two preceding steps. Thanks to this, it became possible to obtain a solution in cases in which the classic SIMP method failed. The variational approach was adopted and compliance was minimized under constraints imposed on body mass. FEM was used to solve numerical examples. The numerical analysis confirmed the effectiveness of the proposed method, particularly for structures with relatively long spans.

Key words: topology optimization, minimum compliance, new incremental method of updating Young's modulus

1. Introduction

The aim of topology optimization is to find an optimum distribution of the material from which a given structure is to be made, in a certain defined area, called a design area, under the prescribed boundary conditions and load. In this paper a variational approach is used for this purpose. The compliance function

$$\Pi^E(x,v) = \int_\Omega X^i v_i \, d\Omega + \int_{\partial\Omega_t} t^i v_i \, ds \tag{1}$$

was minimized under the constraints imposed on body mass, i.e. the quantity of available mass did not change in the course of optimization and in each successive step the same amount of mass would be distributed within the design area:

$$m_j = m_0 \tag{2}$$

where

$$m_0 = a\, m, \qquad 0 < a < 1 \quad \text{and} \quad m = V\, r_0 \tag{3}$$

j stands for the number of a consecutive optimization step and m_j is the body mass in the optimization step, m_0 – the quantity of available mass, a – a mass reduction coefficient defining what proportion of the mass located in the design area is used in the optimization process, r_0 – the density of the material from which the structure is to be built and V – the volume of the design area.

The optimization process would lead to a solution for which the value of the strain energy accumulated in the body was minimum. The obtained solutions have the form of: a material/void distribution (a) or a distribution where besides the material/void there is also material whose density is slightly varied and slightly lower than that of the material from which the structure is made (b). Graphically, case (a) is represented as black and white distribution and case (b) as a black and white distribution with shades of grey.

As part of this research the SIMP method Ref. [1, 2, 3] has been improved whereby it has become more effective and useful. The improvement consists in a new way of updating Young's modulus, which implies that it was necessary to develop a new updating procedure.

In the classic SIMP method, Young's modulus in a considered point (finite element) of the body depends on the material density in this point in the preceding optimization step (bearing the number j-1):

$$E_j = E_0 \left(\frac{r_{j-1}}{r_0} \right)^p \tag{4}$$

where E_j is the Young modulus in the current step (j), E_0 is the Young modulus of the material from which the structure is to be built and r_{j-1} is the preceding step material density relative to that of current step j. In the proposed method, the Young modulus in a considered finite element in the j-th optimization step depends on the element's material density in the preceding step and also on the increment in this element's density between steps j-1 and j-2. The increment is additionally scaled through parameter a. The increment so formulated is defined as d

$$d = \frac{r_{j-1} - r_{j-2}}{a} \tag{5}$$

and it is added or subtracted from the preceding step material density:

$$E_j = E_0 \left(\frac{r_{j-1} + d}{r_0} \right)^p \tag{6}$$

$$E_j = E_0\left(\frac{r_{j-1} - d}{r_0}\right)^p \tag{7}$$

The algorithm with updating according to eq. (6) is further referred to as Alg+ while the one with updating according to eq. (7) is referred as Alg–. Since the proposed algorithm uses densities from the step whose number is lower by 2 than the number of the considered step, it can be introduced starting with the step whose number is (j≥2) according this scheme:

Step 0 Step 1

$$E_{j=0} = E_0\,, \quad E_{j=1} = E_0\left(\frac{r_{j=0}}{r_0}\right)^p\,,$$

Step 2 Step 3 (…)

$$E_{j=2} = E_0\left(\frac{r_{j=1} \pm d}{r_0}\right)^p\,, \quad E_{j=3} = E_0\left(\frac{r_{j=2} \pm d}{r_0}\right)^p\,, (\ldots). \tag{8}$$

As it is apparent, the proper updating relation is the same for steps no. 2, 3, etc., which is denoted by (…).

2. Numerical examples

A program based on the above algorithm was written in *Matlab*. Then its effectiveness was checked: by adjusting (increasing) parameter *a*, solutions identical with the classic SIMP solution would be obtained and by reducing this parameter, solutions in the cases in which the classic SIMP method yielded no solution were obtained.

The solutions obtained using the proposed incremental method are compared below with the ones yielded by the classic SIMP method. The latter solutions were obtained using a program called Alg_1 (differing in only the updating procedure from Alg– and Alg+) developed by the authors. Consequently, the comparative analysis is even more reliable and its conclusions can be useful in the further search for more effective topology optimization algorithms.

The Alg_1 algorithm used in the numerical program had been previously tested Ref. [4]. In part it is based on Ref. [5] where threshold functions (among other things) were used to speed up the process of obtaining the optimal solution.

The numerical examples provided are typical literature benchmarks, i.e. a freely supported beam and a cantilever. The aim of this approach was to ensure high comparability with the results reported in the literature. A freely supported beam fixed in two ways is considered (Fig. 1). In scheme 1 (*Sch. 1*), two constrains on the left support and one constraint on the right support have been removed. In scheme 2 (*Sch. 2*), two constraints have been removed on each of the supports. The beams are loaded with force *P* at midspan on the upper edge. The third scheme (*Sch. 3*) represents a cantilever with its left edge fixed, loaded with force *P* in the middle of its height.

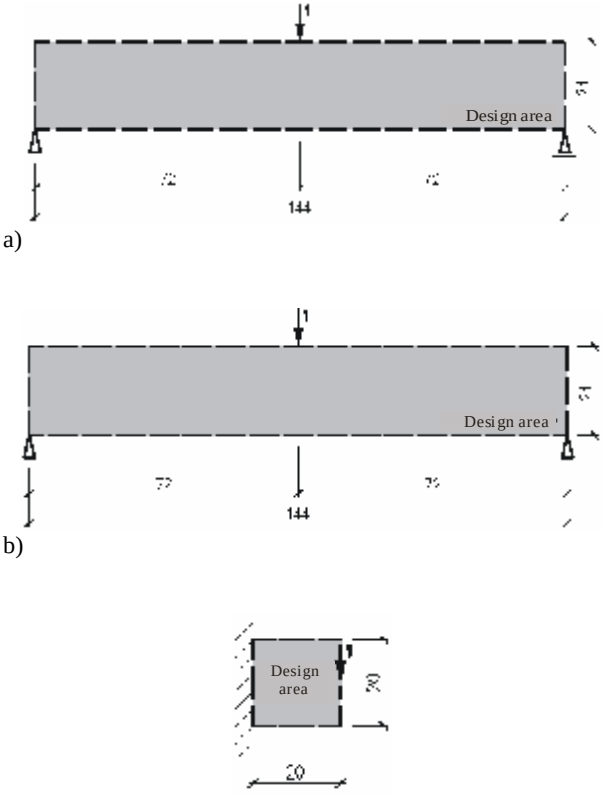

Figure 1: Static schemes of considered cases: freely supported beam (*Sch. 1* a), *Sch. 2* b)), and cantilever c).

A comparison of strain energy for the cases shown in Fig. 2a and Fig. 2b shows that the Alg+ algorithm yielded strain energy values lower than the ones yielded by Alg_1 at decreasing parameter *a*. The further reduction of parameter *a* did not lead to a more satisfactory solution (a more optimal topology). The value of parameter *a*, the number of the step in which the topology was obtained and the strain energy value are shown above each topology. The value of exponent *p* (Eqn.. (6) and Eqn (7)), the lower density bound, the value of the mass reduction coefficient *a*, and the form of the threshold function (in which *nk* stands for the number of the optimization step) are given at the top of the figure. It is apparent that the threshold function value depends on the number of the current optimization step, which substantially stabilizes the optimization process and as the step number increases the material removed from the less strained elements has an ever greater density. In other words, thanks to the threshold function the material can be removed gradually and smoothly (initially the material with a relatively low density is removed and then at an ever higher step number, increasingly denser material is removed). If a too high threshold function value were used in the first steps, the material would be removed from some elements too quickly and the obtained topology would be quite irregular whereby its strain energy (*en*) would be quite high, which means that the topology would not be optimal in comparison with the topology obtained using the "gentle" threshold function. The analyzed quantities are expressed as dimensionless. A 144x24 FE mesh was adopted for *Sch. 1* and *Sch. 2* and a 20x20 mesh was used for *Sch. 3*.

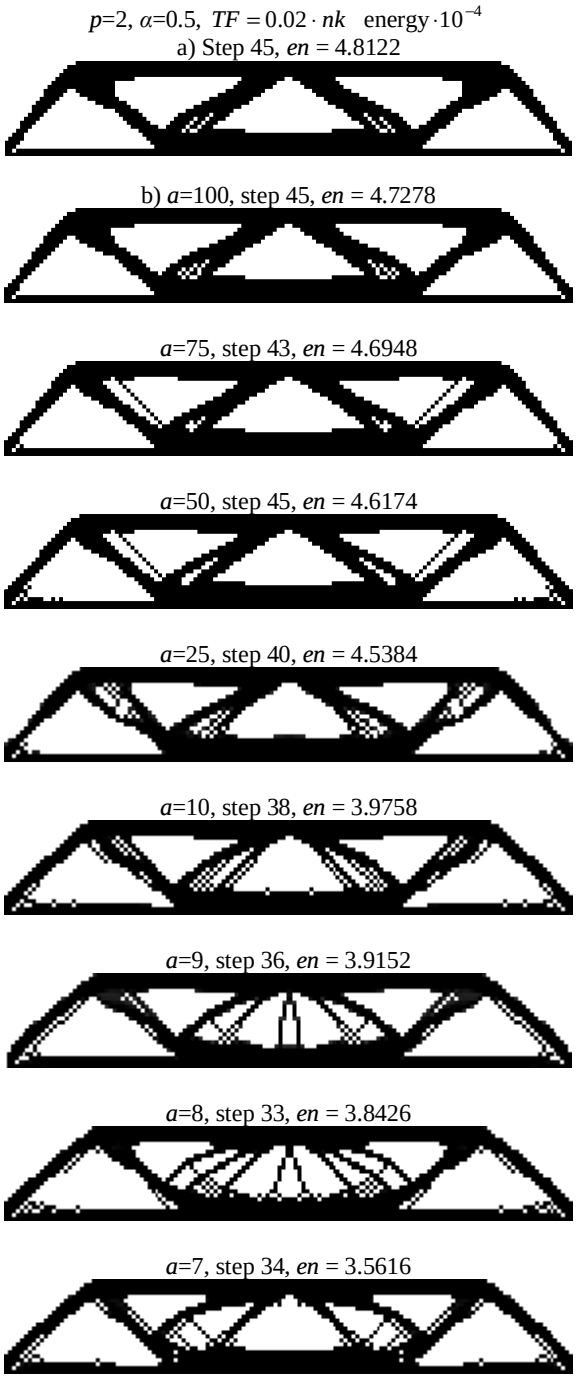

Figure 2: Topologies obtained for *Sch 1* and p=2, using algorithm Alg_1 (a) and Alg+ (b).

Figure 3 shows (in the same way as Fig. 2) computation results for *Sch. 3*. Similar trends are observed, but it was found that if parameter a decreases too much, this may result in an increase in the strain energy determined for this topology.

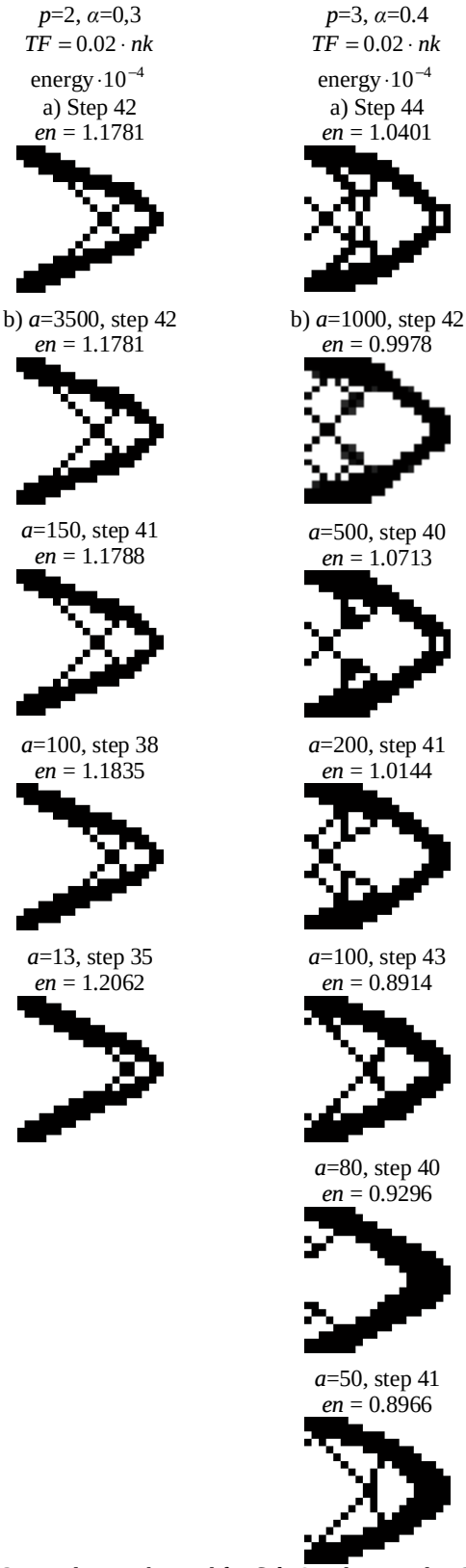

Figure 3: Topologies obtained for *Sch. 3* and p=2 and p=3, using algorithm Alg_1 (a) and Alg+ (b).

Since no solution is obtained when a too low (below 13) value of parameter a is used, empty space is left in the left column in Fig. 3.

Exemplary topologies yielded by Alg– are shown below the ones yielded by Alg+. The observed trends concerning topologies and their energies are similar in the two cases.

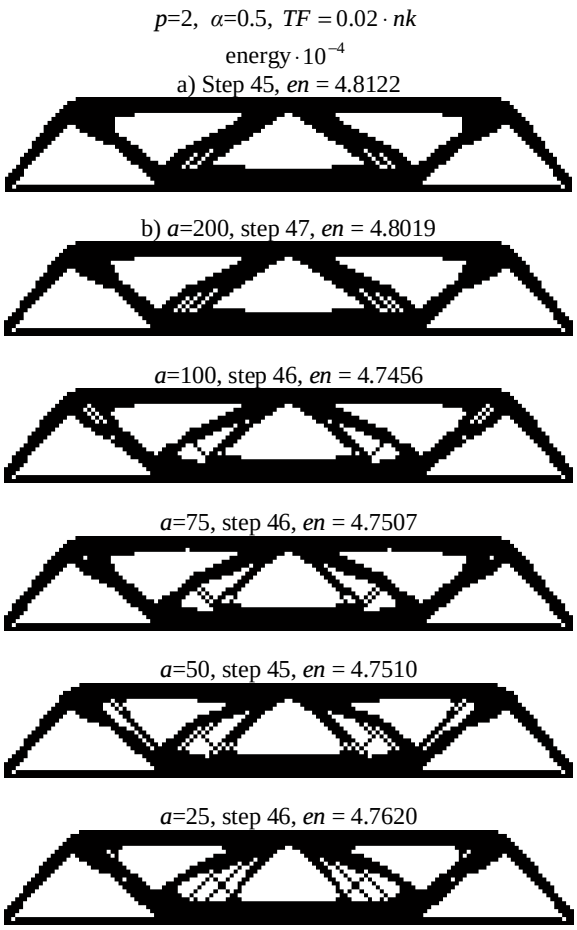

Figure 4: Topologies obtained for *Sch. 1* and p=2, using algorithm Alg_1 (a) and Alg– (b).

2.1. Results for different exponent values - p

In this subsection, exemplary topologies obtained for different values of exponent p in Eqs (6, 7) are analyzed. First of all, solutions with higher exponent values are subjected to scrutiny since exponents with a value higher than 3 are seldom used in the literature. Higher exponent values result in the relatively quicker removal of material from the relatively less strained areas in which relatively lower strain energy has accumulated. When the incremental method is used, material is removed from the less strained areas not so quickly and precisely as in the case of the classic SIMP method, but more optimal topologies are obtained.

As an illustration, Fig. 5 shows the solutions obtained for exponent $p = 4$ and mass reduction coefficient $a = 0.5$. Fig. 5c shows the topology obtained in step 47 by means of program Alg–. No acceptable topology was obtained for exponent $p = 4$, using either Alg_1 (Fig. 5a) or Alg+ (Fig. 5b). It appears that increment addition or subtraction is of considerable significance since it favourably affects the rate and way of material removal from the less strained elements in the design area. In the cases shown in Fig. 5a and 5b, the topologies were obtained in step 11. No changes were observed in the next steps.

Figure 5: Topologies obtained for p=4 and a=0.5, using Alg_1 a), Alg+ b) and Alg– c).

Similar results were obtained for p=5 (Fig. 6). Also here the Alg+ algorithm yielded no solution.

Figure 6: Topologies obtained for p=5 i a=0.45, using Alg_1 a) and Alg– (step 47) b).

Similar analyses as for the freely supported beam were carried out for cantilever *Sch 3*. The results obtained by means of Alg_1and Alg+, and Alg_1 and Alg– are compared in respectively Fig. 7 and Fig. 8. The more refined topology characterized by lower strain energy, shown in Fig. 7, was obtained using Alg+ and the one in Fig. 8 by means of Alg–.

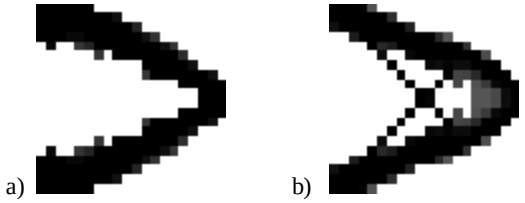

Step 52, *en*=1.115 Step 27, *en*=0.838

Figure 7: Topologies obtained for p=3 and a=0.4, using Alg_1 a) and Alg+ b).

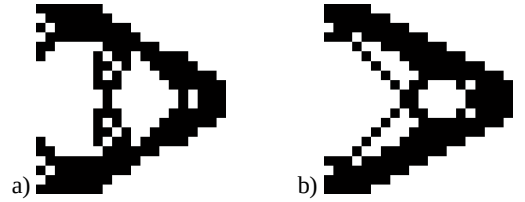

Step 79, *en*=1.113 Step 76, *en*=0.935

Figure 8: Topologies obtained for p=5 and a=0.4, using Alg_1 a) and Alg– b).

2.2. Results for different FE mesh densities

In order to further check the effectiveness of the incremental algorithms, the latter were tested for different FE mesh densities and the results were compared with the ones obtained using Alg_1. Figure 9 shows the topologies yielded by the Alg_1 algorithm for *Sch. 1* under the same control parameters, three different FE mesh densities (72x12, 144x24, 288x48) and a constant 144x24 [m] design area.

p=1, $TF = 0.02 \cdot nk$, α=0.5, $\boldsymbol{a}$=1000, energy$\cdot 10^{-4}$

a) 72x12 elements with side 2.0m (144x24 [m])
Step 46, *en*=4.7716

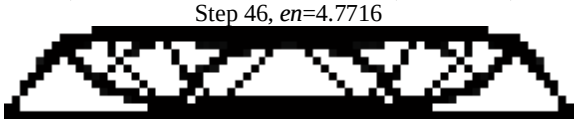

b) 144x24 elements with side 1.0m (144x24 [m])
Step 40, *en*=4.7059

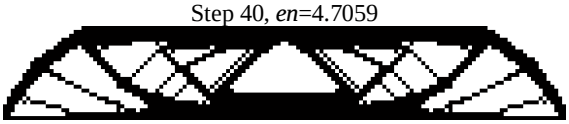

c) 288x48 elements with side 0.5m (144x24 [m])
Step 38, *en*=4.6131

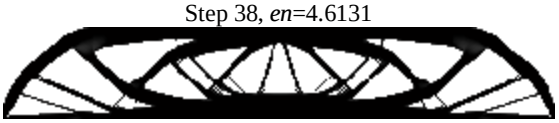

Figure 9: Topologies obtained using Alg– and *Sch. 1*

p=1, $TF = 0.02 \cdot nk$, α=0.5, $\boldsymbol{a}$=1000, energy$\cdot 10^{-4}$

a) 72x12 elements with side 2.0m (144x24 [m])
Step 36, *en*=4.7572

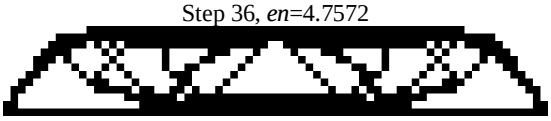

b) 144x24 elements with side 1.0m (144x24 [m])
Step 31, *en*=4.5489

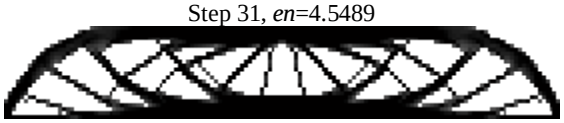

c) 288x48 elements with side 0.5m (144x24 [m])
Step 41, *en*=4.5995

Figure 10: Topologies obtained using Alg+ and *Sch. 1*.

Similar results obtained by means of Alg+ are shown in Fig. 10. Obviously, the results obtained for the densest mesh have the smoothest shapes. It sometimes happens that the strain energy for the densest mesh solution is somewhat greater than for a less dense mesh. This is due to, among other things, the fact that although the topology obtained in such a case is smooth, it is at the same time more compliant. This can be sometimes directly seen when one examines the particular structural components (e.g. in the fixing region, where too much material was removed in the course of optimization, whereby the structure is more compliant).

In order to provide a wider analytical spectrum, Fig. 11 shows the topologies obtained for *Sch. 3* and the parameters specified in the figure.

p=1, $TF = 0.015 \cdot nk$
α=0.3
energy$\cdot 10^{-4}$

10x10 elements with side 2.0m
(20x20 [m])
Step 46
en=1.3966

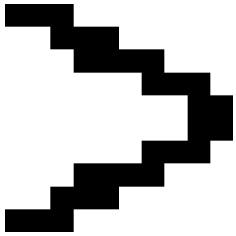

20x20 elements with side 1.0m
(20x20 [m])
Step 53
en=1.2026

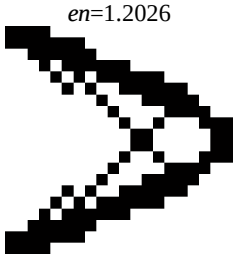

40x40 elements with side 0.5m
(20x20 [m])
Step 57
en=1.1451

Figure 11: Topologies obtained using Alg_1.

In the case of the initial algorithm (Alg_1) it is apparent that the topologies obtained for the different FE mesh densities differ considerably from each other. For the 10x10 mesh the topology has a simple shape and a high strain energy value. When the mesh density was increased (to 20x20), a refined shape with a cross reinforcing the structure was obtained whereby the strain energy value is much lower. However, for the densest mesh (40x40) the cross is smaller and it is located closer to the load application region. Also additional bars have appeared in the vicinity of the supports and the strain energy value is the lowest from among the three meshes used for Alg_1.

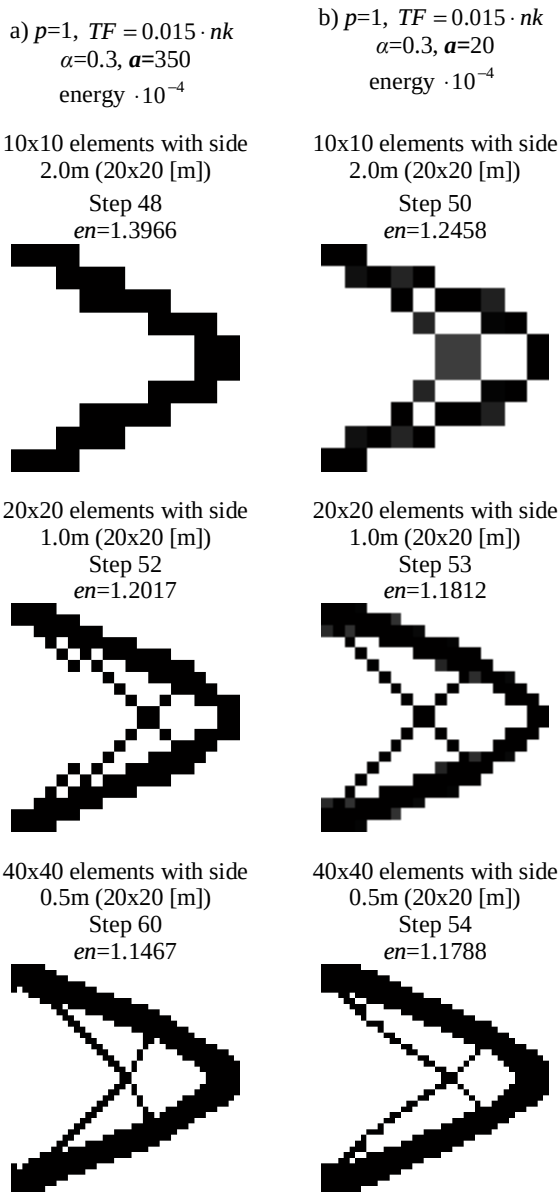

Figure 12: Topologies obtained for different values of control parameters *a:* $a = 350$ a) and $a = 20$ b), using Alg–.

When Alg– with control parameters $a = 350$ and $a = 20$ was used the similarity between the topologies at the different mesh densities significantly increased (Fig. 12). In the case of $a = 350$ and the 10x10 mesh a topology identical as the one yielded by Alg_1 was obtained. Whereas the topology obtained for the 20x20 mesh is very similar to the one yielded by the initial algorithm (Alg_1), except that for Alg– a material-void distribution and a slightly lower strain energy value were obtained. At the densest mesh (40x40) a topology with a cross similar in shape to the one in the 20x20 mesh topology was obtained. It should be noted that this topology has the lowest strain energy value from among all the considered topologies obtained using the incremental method. In the case of $a = 20$, topologies with a cross reinforcing the structure were obtained for all the mesh densities. For the 10x10 mesh the cross is responsible for the much lower strain energy value than in the case of Alg_1 and Alg+, but the material distribution is not of the material-void type. The topology obtained for the 20x20 mesh is characterized by a lower strain energy value than in the case of the other algorithms.

To sum up, it should be noted that better solution convergence at different mesh densities was achieved when algorithms Alg+ and Alg– were used. Although, as shown above, in one case Alg+ was yielded better results while in another case Alg– performed better. This depends on the particular case and the assumed design parameters. In some cases, the initial algorithm yields a slightly better result. Thanks to the increment based on parameter ***a*** it is possible to search for a more optimal solution than the one yielded by the initial algorithm (Alg_1) while preserving better stability of shape similarity when FE mesh density is changed.

2.3. Results for different ratios of design area sides

Another subject of the analysis were solutions for large spans of beams *Sch. 1*, *Sch.* 2 and *Sch. 3*. In the first two cases, the span between the supports was considerably increased while in the third case the length of the cantilever was considerably increased. Computations were performed using the initial algorithm (Alg_1) and algorithms Alg+ and Alg–.

First a 240x24 [m] (a 10:1 side ratio) *Sch. 1* beam was analyzed (Fig. 13). The computations were performed for a quite low (for this scheme) value of mass reduction coefficient $a = 0{,}35$. In the case of the incremental method, controlling parameter $a = 7000$ was used. As shown below, the topology yielded by Alg_1 is characterized by the highest strain energy value (due to the unoptimal shape). Algorithm Alg+ yielded a topology with a better arrangement of the branches and a considerably lower strain energy value. The qualitatively best result (with the most well-defined shape and the lowest strain energy value) was yielded by Alg–.

Then a 480x24 (20:1) *Sch. 2* beam was analyzed (Fig. 14). The topologies yielded by respectively Alg_1 and the incremental method for two different control parameter values: $a = 1000$ and $a = 500$ are compared below. In the case of Alg_1, the topology has a poorly refined and unoptimal shape and a very high strain energy value. When Alg+ was used, two better (more openwork) topologies with a lower strain energy value than in the case of Alg_1 were obtained. The topologies yielded by Alg– also show lower strain energy values than the ones yielded by Alg_1. All the topologies are qualitatively good and contain a small number of elements in shades of grey. One should also note how the structure is shaped in the support region, i.e. in the bottom corners of the design area. As the span was increased, a certain amount of material accumulated in the support region.

a) step 46, *en*=0.0038

b) step 27, *en*=0.0026

c) step 40, *en*=0.0025

Figure 13: Topologies obtained using Alg_1 a), Alg+ b) and Alg– c).

a) Step 43, *en*=0.0068

b) Step 31, *en*=0.0063, *a*=1000

Step 33, *en*=0.0062, *a*=500

c) Step 44, *en*=0.0063, *a*=1000

Step 44, *en*=0.0064, *a*=500

Figure 14: Topologies obtained using Alg_1 a), and incremental algorithms ($a = 1000$, $a = 500$): Alg+ b) and Alg– c).

a) Step 58, *en*=0.0079

b) Step 62, *en*=0.0060

Figure 15: Topologies for *p*=1, *a*=1000 and *a*=0.5, obtained using Alg_1 a) and Alg– b).

a) Step 31, *en*=0.0059

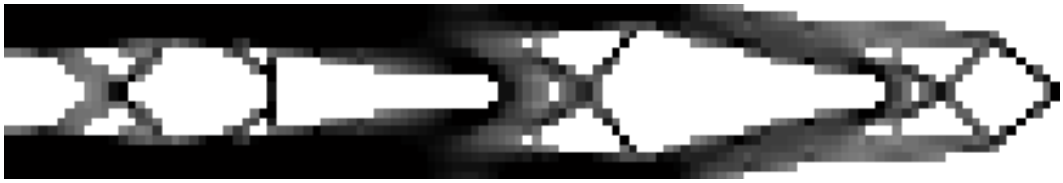

b) Step 57, *en*=0.0062

Figure 16: Topologies for p=1 a=10000 and a=0.5, obtained using Alg+ a) and Alg– b).

Finally, the cantilever scheme was analyzed. The design area was 120x20 [m], i.e. it had a side ratio of 6:1. Figure 15 shows one of the two considered cases. As one can see, an interesting, original shape of the structure has been obtained and the strain energy value is lower in the case of Alg–. In the other case, the cantilever with slightly changed design parameters was analyzed (Fig. 16). The comparison shows that using the Alg– algorithm with a proper value of parameter a one can obtain a result which could not be obtained by means of the initial algorithm (Alg_1). In the case of Alg_1, the topology was obtained in step 31 when the optimization processes ended. The topology is characterized by a large number of elements with shades of grey. In the case of Alg+, there is practically no improvement relative to the initial algorithm. The topology is only slightly different in the support region where a somewhat different framework scheme has appeared. The computation process, similarly as in the case of Alg_1 is stopped in step 31. The topology yielded by Alg– is very similar in its arrangement of branches to the one obtained using Alg_1, but the final distribution is very close to black and white. Thus one can say that the use of Alg– helped to improve process convergence and to obtain a topology with a black and white distribution.

To sum up, thanks to the application of the incremental method to design areas in which one of the dimensions is much larger than the other one (e.g. the spans of long bridges of low height or long-reach cantilevers), qualitatively better topologies were obtained. Sometimes the incremental method yielded a topology when the initial algorithm (Alg_1) failed to yield one. It should be noted that the Alg– algorithm is much more computationally effective.

3. Conclusions

The incremental method, which in the Young modulus updating algorithm takes into account a change in mass density in the particular finite elements in the last two steps of the optimization process, represents a significant extension to the SIMP algorithm (Alg_1). The change, i.e. an increment in density, can be taken into account by adding (Alg+) or subtracting (Alg–) the increment value.

The analyses concerning the strain energy level of the obtained topologies, the use of different FE mesh densities and the application of the incremental method to design areas with a large difference in the length of their sides have shown that the use of the incremental method helps to obtain energywise desirable refined shapes. It has also been demonstrated that the use of increments (particularly in the case of Alg–) has a positive effect on computations involving high powers, by improving optimization process convergence. The algorithms (Alg+, Alg–) improved in this way enable the search for qualitatively and energywise better topologies in cases when the initial algorithm fails or yields unoptimal solutions.

To sum up, the proposed incremental method of updating Young's modulus yields better results than the classic SIMP method. The topologies obtained in this way are characterized by a lower strain energy level and are better, i.e. more refined. In particular, better results are obtained for:

1. higher values of the exponent in Eqn. 6 and 7,
2. high ratios of design area sides.

Thanks to the use of the incremental method a better convergence of the topology optimization process is achieved.

References

[1] Bendsøe, M.P., Optimal shape design as a material distribution problem, *Struct. Optim.,* 1, pp. 193-202, 1989.

[2] Bendsøe, M.P. , and Sigmund, O., *Topology optimization, theory, methods and applications*. Springer, Berlin Heidelberg New York, 2003.

[3] Ramm, E., Bletzinger, K.-U., Reitinger, R. and Maute, K., The challenge of structural optimization. In: Topping B H V, Papadrakakis M (ed) Advanced in Structural Optimization (Int. Conf. on Computational Structures Technology held in Athen), pp. 27-52, 1994.

[4] Kutyłowski, R. and Rasiak, B., Influence of various design parameters on the quality of optimal shape design in topology optimization analysis, *Proceedings in Applied Mathematics and Mechanics,* 8, pp. 10797-10798, 2008.

[5] Kutyłowski, R., On nonunique solutions in topology optimization, *Struct. Mult. Optim.*, 23, pp. 389-403, 2002.